European Journal of Pharmaceutical Sciences 185 (2023) 106441

Contents lists available at ScienceDirect

European Journal of Pharmaceutical Sciences

journal homepage: www.elsevier.com/locate/ejps

Research Article

Phosphodiesterase (PDE) 4 inhibition boosts Schwann cell myelination in a 3D regeneration model

Melissa Schepers [a,b,c,1], Afonso Malheiro [d,1], Adrián Seijas Gamardo [d], Niels Hellings [b,c], Jos Prickaerts [a], Lorenzo Moroni [d], Tim Vanmierlo [a,b,c,2,*], Paul Wieringa [d,2]

[a] Department Psychiatry and Neuropsychology, European Graduate School of Neuroscience, School for Mental Health and Neuroscience, Maastricht University, Maastricht, MD 6200, the Netherlands
[b] Biomedical Research Institute, Hasselt University, Hasselt 3500, Belgium
[c] University MS Center (UMSC) Hasselt-Pelt, Hasselt, Belgium
[d] MERLN Institute for Technology-Inspired Regenerative Medicine, Maastricht University, the Netherlands

A B S T R A C T

Phosphodiesterase 4 (PDE4) inhibitors have been extensively researched for their anti-inflammatory and neuroregenerative properties. Despite the known neuroplastic and myelin regenerative properties of nonselective PDE4 inhibitors on the central nervous system, the direct impact on peripheral remyelination and subsequent neuroregeneration has not yet been investigated. Therefore, to examine the possible therapeutic effect of PDE4 inhibition on peripheral glia, we assessed the differentiation of primary rat Schwann cells exposed *in vitro* to the PDE4 inhibitor roflumilast. To further investigate the differentiation promoting effects of roflumilast, we developed a 3D model of rat Schwann cell myelination that closely resembles the *in vivo* situation. Using these *in vitro* models, we demonstrated that pan-PDE4 inhibition using roflumilast significantly promoted differentiation of Schwann cells towards a myelinating phenotype, as indicated by the upregulation of myelin proteins, including MBP and MAG. Additionally, we created a unique regenerative model comprised of a 3D co-culture of rat Schwann cells and human iPSC-derived neurons. Schwann cells treated with roflumilast enhanced axonal outgrowth of iPSC-derived nociceptive neurons, which was accompanied by an accelerated myelination speed, thereby showing not only phenotypic but also functional changes of roflumilast-treated Schwann cells. Taken together, the PDE4 inhibitor roflumilast possesses a therapeutic benefit to stimulate Schwann cell differentiation and, subsequently myelination, as demonstrated in the biologically relevant *in vitro* platform used in this study. These results can aid in the development of novel PDE4 inhibition-based therapies in the advancement of peripheral regenerative medicine.

1. Introduction

Peripheral demyelinating neuropathies arising from pathological processes or trauma can lead to severe neuropathic pain, as well as motor and sensory deficits (Balakrishnan et al., 2020). Peripheral nervous system (PNS) white matter tracts comprise of myelinated axons. In the PNS, the myelin-producing glial support is provided by Schwann cells, whereas oligodendroglial cells maintain myelination in the CNS (Balakrishnan et al., 2020; Jessen, 2004). Besides their myelinating properties, Schwann cells play a crucial role in nerve regeneration following PNS neuropathies as they actively support nerve repair by secreting trophic factors and cytokines that promote neuroregeneration and axonal outgrowth (Balakrishnan et al., 2020). However, upon aging and disease, Schwann cell dysfunction limits its regenerative capacity, hampering PNS repair (Balakrishnan et al., 2020). Hence, there is a growing need to identify novel pharmacological targets capable of restoring Schwann cell function and, thereby nerve repair.

The second messenger cyclic adenosine monophosphate (cAMP) has been shown to be crucially involved in Schwann cell biology (Han et al., 2019). Both Schwann cell differentiation and the subsequent myelination processes are positively regulated by cAMP, where prolonging or elevating intracellular cAMP signaling has been demonstrated to increase both the expression of myelin proteins (*e.g.* MAG, MBP and O1) and the Krox-20/c-Jun transcription factor ratio towards favouring Schwann cell differentiation and myelination (Balakrishnan et al., 2020; Bacallao and Monje, 2015; Jessen et al., 1991; Monje et al., 2010; Guo et al., 2012; Knott et al., 2014; Parkinson et al., 2008; Monje et al., 2009; Morgan et al., 1991; Han et al., 2023). The importance of cAMP in

* Corresponding author at: Department Psychiatry and Neuropsychology, European Graduate School of Neuroscience, School for Mental Health and Neuroscience, Maastricht University, Maastricht, MD 6200, the Netherlands.
E-mail address: tim.vanmierlo@uhasselt.be (T. Vanmierlo).
[1] Shared first authors
[2] Shared last authors

https://doi.org/10.1016/j.ejps.2023.106441
Received 16 November 2022; Received in revised form 14 March 2023; Accepted 29 March 2023
Available online 31 March 2023

Schwann cell biology is reinforced by the results obtained with forskolin, a potent agonist of the cAMP anabolic membrane-bound catalyst adenylyl cyclase. Depending on the concentration of forskolin, and therefore cAMP, either Schwann cell proliferation or differentiation was stimulated (Yamada et al., 1995; Glenn and Talbot, 2013; Monje, 2015). In line, following peripheral transection and crush injuries *in vivo*, cAMP levels are reduced up to 10% in Schwann cells and only start to normalize upon the initiation of remyelination, rendering the spatio-temporal control of cAMP signaling essential for proper Schwann cell functioning (Walikonis and Poduslo, 1998).

The tight control of intracellular cAMP levels is accomplished by a family of cAMP-degrading enzymes called phosphodiesterases (PDEs). In neural tissue, the PDE4 family actively limits cAMP levels in both neural and glial cells, accounting for 70 to 80% of the complete PDE expression profile (Tibbo et al., 2019; Nikulina et al., 2004). In the CNS, inhibiting PDE4 enhances oligodendrocyte precursor cell (OPC) differentiation and subsequent remyelination, indicating a central role for PDE4 in the (re)myelination process (Syed et al., 2013; Sun et al., 2012; Schepers et al., 2023). In the PNS, regulating intracellular cAMP levels via inhibition of PDE4 has been mainly investigated for its potential neuroregenerative properties. Despite the inhibitory microenvironment following PNS nerve damage, elevating cAMP with the PDE4 inhibitor rolipram promoted *in vivo* axonal outgrowth across the lesion site (Udina et al., 2010). However, the effect of PDE4 inhibition on Schwann cells remains speculative and is based on *in vivo* results or findings with cAMP analogues.

In this study, we aimed to determine the therapeutic potential of the PDE4 inhibitor roflumilast on Schwann cell differentiation and myelination. Using primary rat Schwann cells, we first evaluated and confirmed the importance of cAMP in promoting cellular differentiation in a 2D culture model. Furthermore, by indirectly increasing intracellular cAMP using roflumilast, Schwann cell differentiation could be promoted as well. Next, to mimic the *in vivo* environment following PNS neuropathies, primary rat Schwann cells were seeded on a 3D peripheral nerve model scaffolds. This creates an analogue of the bands of Büngner, which are longitudinally aligned Schwann cells tracks that are formed in the initial stages of PNS repair to guide axonal regrowth (Malheiro et al., 2020). In line with the 2D culturing conditions, roflumilast promoted Schwann cell differentiation within the 3D model as indicated by the increased gene expression and protein levels of myelin-related proteins. Finally, to evaluate myelination and axonal growth, we co-cultured rat Schwann cells with human iPSC-derived neurons in a newly established and validated 3D culture platform (Malheiro et al., 2021). Schwann cells treated with roflumilast positively influenced nerve repair reflected by an accelerated axonal growth. Furthermore, roflumilast treated Schwann cells demonstrated an increased differentiation and subsequent myelination of newly formed iPSC-derived nociceptive neurons. The findings of this study demonstrate for the first time the therapeutic potential of PDE4 inhibition on PNS remyelination and nerve repair, and can therefore aid in the development of novel regenerative therapeutic strategies.

2. Material and methods

2.1. 3D scaffold fabrication for Schwann cell culturing

The 3D scaffolds were fabricated via a two-step electrospinning (ESP) process with a custom-built apparatus. First, a release layer was produced by electrospraying a solution of 50% polyethyleneoxide (PEO, Mn = 3350, Sigma-Aldrich, Catalog #P5413) in Milli-Q onto aluminum foil. For this, the solution flowed through a 0.8 mm inner diameter stainless steel needle (Unimed S.A.) at 2 ml/hr, while subjected to 20 kV and at a distance of 10 cm from a 60 mm diameter mandrel rotating at 5000 rpm. Afterwards, a nonwoven polyurethane mesh (6691 LL (40 g/m2), a kind gift from Lantor B.V., The Netherlands) was prepared by punching an array of 12 mm circular holes and placed on the mandrel, covering the PEO sprayed-foil. Next, the scaffolds were produced by ESP of 300PEOT55PBT45 (PolyVation) in 75:25 Chloroform/1,1,3,3-hexafluoroisopropanol solution onto the mesh support structure. For this process, the solution flowed through a 0.5 mm inner diameter stainless steel needle (Unimed S.A.) at 0.75 ml/hr, while applying a voltage of 12 kV and at a distance of 10 cm from a rotating mandrel (at 5000 rpm). During both processes, the humidity remained at 35–40% and the temperature at 22–24 °C. Finally, individual scaffolds were generated from the polyurethane mesh by punching 15 mm-outer diameter sections concentric to the 12 mm holes, resulting in a thin ESP membrane supported by a polyurethane mesh ring. Next, scaffolds were dipped in deionized water to allow detachment of the scaffolds and stored in PBS. Preceding the cell seeding, scaffolds were sterilized by immersing them in 70% ethanol for 1 h, followed by a repeated PBS washing step.

2.2. Primary Schwann cells harvesting, purification and culture

Primary Schwann cells were harvested from the sciatic nerves of neonatal Wistar rat pups, following local and Dutch animal use guidelines, and were based on previously described protocols (Malheiro et al., 2020; Malheiro et al., 2021; Kaewkhaw et al., 2012). Briefly, nerve segments were extracted and digested in a 0.05% collagenase solution (60 min, 37 °C, 5% CO_2)(Sigma-Aldrich, Catalog #C9697). Cell suspensions were passed through a 40 μm cell strainer, washed and seeded on 35 mm poly-L-lysine (0.01%; Sigma-Aldrich, Catalog #P1666) and 1 μg/ml laminin (R&D systems, Catalog #3400–010–02) pre-coated petridishes in proliferation and purification medium (DMEM D-valine (Cell Culture Technologies), 2 mM L-glutamine (ThermoFisher Scientific, Catalog #25,030,081), 10% (v/v) foetal bovine serum (FBS)(Catalog #F3297), 1x N2 supplement (R&D Systems, Catalog #AR003), 20 μg/ml bovine pituitary extract (Catalog #P1476), 5 μM forskolin (Catalog #93,049), 100 U/ml penicillin and 100 μg/ml streptomycin (Catalog #P4458), and 0.25 μg/ml amphotericin B (Catalog #PHR1662)(all Sigma-Aldrich unless stated otherwise). Fresh medium was added at day 7 of culture and changed every two days until confluency. Cells were used between passage number 3 and 6 (P3-P6).

2.3. 2D Schwann cell culture

Schwann cells were seeded at 25×10^3 cells/cm^2 on glass coverslips (12 mm; in a 24 well plate) (immunocytochemistry) or 24-well plates (qPCR), both pre-coated overnight with 1 μg/ml laminin-1 (R&D systems, Catalog #3400–010–02) and 2 μg/ml poly-D-lysine (Sigma-Aldrich, Catalog #A-003-E). The seeding medium was composed of DMEM supplemented with 10% FBS (v/v) (Sigma-Aldrich, Catalog #F3297). After 24 h of culture, the medium was changed to serum deprivation medium (1% FBS (v/v)). To evaluate the effect of cAMP supplementation on Schwann cell differentiation, medium was changed after 24 h to serum-deprived DMEM medium containing 250 μM of 8-(4-Chlorophenylthio)adenosine 3′,5′-cyclic monophosphate sodium salt (CPT-cAMP, water soluble, Sigma-Aldrich, Catalog #C3912). Cells were cultured in these conditions for 3 days and either fixated with 4% PFA for 20 min (immunocytochemistry) (Sigma-Aldrich, Catalog #158,127) or lysated with Qiazol (qPCR)(Qiagen, Catalog #79,306). To evaluate the effect of the PDE4 inhibitor roflumilast on Schwann cell differentiation, roflumilast (DMSO soluble, BioLeaders) was supplemented instead of CPT-cAMP 24 h following serum deprivation (1/1000 final DMSO fraction in cultures) at a concentration of 5 μM or 10 μM (IC50 ranges between 0.2 and 4.3 nM in cell free assay) (Hatzelmann et al., 2010). For downstream signaling pathway analysis, Schwann cells were treated with 250 μM db-cAMP (Bio-techne, Catalog #1141) or 10 μM roflumilast, with or without the EPAC inhibitor ESI-09 (10 μM) (Bio--techne, Catalog #4773) or the PKA inhibitor H-89 (10 μM) (Bio-techne, Catalog #2910). Cells were kept in culture for six days and treatment was repeated on day 2 and 4 (with a 50% medium change). Cells were

fixated with 4% PFA for 20 min (immunocytochemistry) or lysated with Qiazol (qPCR). Based on DAPI counts, roflumilast did not affected cell survival or proliferation at the used dosages (data not shown).

2.4. 3D Schwann cell culture

Schwann cells were seeded at 100 × 10^3 cells per scaffold (above-mentioned) and cultured in Schwann cell medium composed of DMEM supplemented with 4 mM L-glutamine (ThermoFisher Scientific), 100 U/ml penicillin and 100 μg/ml streptomycin (ThermoFisher Scientific, Catalog #25,030,081), 10% (v/v) FBS (Sigma-Aldrich, Catalog #F3297), 20 μg/ml bovine pituitary extract (Sigma-Aldrich, Catalog #P1476), 5 μM forskolin (Sigma-Aldrich, Catalog #93,049) and 1x N2 supplement (R&D systems, Catalog #AR003). After 7 days of culturing, treatment was initiated by supplementing Schwann cell medium with either vehicle (1/1000 DMSO) or roflumilast. Treatment was repeated every other day after which cells were fixated with 4% PFA for 20 min (immunocytochemistry) or lysated with Qiazol (qPCR) at day 6 of the experiment. Throughout the experiment, cells were kept at 37 °C with 5% CO_2.

2.5. Agarose microwell platform fabrication

A 3% (w/v) sterile agarose (ThermoFisher Scientific, Catalog #16,500,500) solution was prepared in PBS (ThermoFisher Scientific, Catalog #10,010,001). Next, 8 mL of the prepared agarose solution was poured onto an in-house produced PDMS stamp with the negative template of 1580 microwells with a diameter of 400 μM. A short centrifugation step removed the air bubbles, after which the agarose plate was allowed to solidify for 45 min at 4 °C. Upon solidification, the agarose blocks were removed and cut in the appropriate size (12 well plate) and subsequently covered with PBS for storage at 4 °C. The day before cell seeding, PBS was replaced by culture media containing Advanced RPMI 1640 media supplemented with 1x Glutamax (ThermoFisher Scientific, Catalog #35,050,061) and kept at 37 °C with 5% CO_2 overnight.

2.6. iPSCs-derived nociceptive neurons

Human iPSC line LUMC0031iCTRL08 (Provided by the LUMC iPSC core facility) was cultured on Geltrex (ThermoFisher Scientific, Catalog #A1569601) coated dishes at a density of 10 × 10^3 /cm^2 in mTESR1 medium (Stem Cell Technology, Catalog #100–1130). To induce iPSC differentiation into nociceptive neurons, a modified protocol published by *Chambers* et al. was used (Chambers et al., 2012). Briefly, 200 undifferentiated iPSCs are seeded onto 400 μm agarose microwells (described above) and forced to settle by introducing a centrifugation step of 2 min at 1200 rpm. Seeding medium was composed of mTESR1 medium supplemented with 10 μM Y-27,632 (Stem Cell Technology, Catalog #72,303) and 0.5% Geltrex (ThermoFisher Scientific, Catalog #A1569601) in suspension. The cellular spheroid is formed after 24 h and a complete medium change was conducted with mTESR1 medium supplemented with 1% DMSO to initiate cell synchronization. The cells were maintained for 72 h in the synchronization medium. Post synchronization, nociceptor differentiation was initiated by changing the medium into dual SMAD inhibition media containing Advanced RPMI 1640 (Thermofisher Scientific, ThermoFisher Scientific, Catalog #12, 633,012) supplemented with Glutamax (ThermoFisher Scientific, Catalog #35,050,061), 100 nM LDN-193,189 (Tocris, Catalog #6053) and 10 μM SB431542 (Tocris, Catalog #1614). The spheres were maintained for 48 h in the dual SMAD inhibition media. Following this, neural crest commitment was induced via media containing Advanced RPMI 1640 supplemented with Glutamax, 3 μM CHIR99021 (Tocris, Catalog #4423) and 1 μM retinoic acid (Tocris, Catalog #0695). The spheres were maintained in the neural crest induction media for 5 days with a full medium change every other day. Following the neural crest induction, spheres were incubated in notch inhibition media, consisting of Advanced RPMI supplemented with Glutamax, 10 μM SU5402 (Tocris, Catalog #3300) and 10 μM DAPT (Tocris, Catalog #2634), for 48 h. Finally, the neurospheres, composed of trunk neural crest cells, were collected and seeded on the scaffolds. Herein, cells were cultured in neural maturation medium for at least 5 days to reach the nociceptor phenotype. The neural medium is composed of Neurobasal Medium (ThermoFisher Scientific, Catalog #21,103,049), 0.5 mM Glutamax (ThermoFisher Scientific, Catalog #35,050,061), 100 U/ml penicillin and 100 μg/ml streptomycin (ThermoFisher Scientific, Catalog #P4458), 100 ng/ml human nerve growth factor (NGF; Sigma-Aldrich, Catalog #H9666), 50 μg/ml ascorbic acid (Sigma-Aldrich, Catalog #BP461), 25 ng/ml human neuregulin-1 type III (NRG-1 SMDF; R&D systems, Catalog #378-SM) and 1x N21 supplement (R&D systems, Catalog #AR008).

2.7. iPSCs-Schwann cell co-culture on 3D scaffolds

Schwann cells were seeded on the 3D scaffolds and cultured with the PDE4 inhibitors as described above. For this experiment, Schwann cells were first exposed to vehicle (1/1000 DMSO) or roflumilast before introducing the iPSC-derived nociceptive neurons. At day 14 of culture in the scaffolds, the iPSCs-derived neurospheres were collected from the agarose mold and seeded on the scaffolds (one neurosphere per scaffold). The cells were cultured in neural medium composed as described above.

2.8. Quantitative polymerase chain reaction (qPCR)

For gene expression analysis, Schwann cells were lysated using Qiazol (Qiagen, Catalog #79,306) from which total RNA was isolated using the isopropanol precipitation method. Next, cDNA synthesis was conducted using the qScript cDNA synthesis kit (Quanta, Catalog #95,048) according to the manufacturer's instructions. Gene expression analysis was performed using a StepOnePlus detection system (Applied Biosystems, USA). The reaction mixture consisted of SYBR Green master mix (Applied Biosystems, Catalog #A25742), 10 μM forward and reverse primers (IDT), nuclease free water and cDNA template (5 ng/μl), up to a total reaction volume of 10 μl. The primer pairs used for amplification are listed below (Table 1). Results were analysed by the comparative Ct method and were normalised to the most stable housekeeping genes, determined by Genorm (*YWHAZ* and *ACTB* for gene expression analysis within CPT-cAMP and roflumilast experiments, *RPL13a* and *PGK1* for the EPAC and PKA inhibitor experiments).

2.9. Immunostaining

Samples were fixed with 4% paraformaldehyde (PFA) for 20 min at room temperature and subsequently permeabilized for 30 min with 0.1% Triton X-100 dissolved in PBS. Next, a blocking step was conducted with a blocking buffer composed of 5% goat serum, 0.05% Tween-20, and 1% bovine serum albumin (Sigma-Aldrich, Catalog #9048–46–8). Primary antibodies were subsequently dissolved in blocking buffer and samples were incubated overnight at 4 °C. Following washing, secondary antibody incubation was done for 2 h at room temperature. DAPI (1:1000, Sigma-Aldrich, Catalog #28,718–90–3) was used to counterstain the nuclei. The primary antibodies used were the following: anti-βIII tubulin (Sigma-Aldrich, Catalog #T8578, 1:500), anti-myelin basic protein, MBP (Thermo Fisher Scientific, Catalog #PA1–46,447, 1:50) and anti-myelin associated glycoprotein, MAG (Abcam, Catalog #ab89780, 1:100), anti-oligodendrocyte marker 1, O1 (Novus Biologicals, Catalog #MAB1327, 1:100), anti-Krox20 (Sigma-Aldrich, Catalog #ABE1374, 1:100), anti-cJun (Cell Signaling Technologies, Catalog #9165S, 1:300), anti-p75 (Alomone Labs, Catalog #ANT-007, 1:50). The used secondary antibodies were the following: goat anti-mouse conjugated with Alexa Fluor 488; goat anti-mouse conjugated

Table 1
Primer sequences for qPCR.

GENE	FORWARD SEQUENCE (5′−3′)	REVERSE SEQUENCE (5′−3′)
Sox10	GCACGCAGAAAGTTAGCC	TGTCACTCTCGTTCAGCAAC
PLP	TCTGCAAAACAGCCGAGTTC	TGGCAGCAATCATGAAGGTG
cJUN	TCCACGGCCACGGCCAACATGCT	CCACTGTTAACGTGGTTCATGAC
MAG	GCTACAACCAGTACACCTTCTC	TGACCTCTACTTCCGTTCCTG
MBP	ACGCGCATCTTGTTAATCCG	AAGTTTCGTCCCTGCGTTTC
Krox20	GCCCCTTTGACCAGATGAAC	GGAGAATTTGCCCATGTAAGTG
BCL2	ATCGCTCTGTGGATGACTGAGTAC	AGAGACAGCCAGGAGAAATCAAAC
Bax	CCAGGACGCATCCACCAAGAAGC	TGCCACACGGAAGAAGACCTCTCG
BDNF	ATAGGAGACCCTCCGCAACT	CTGCCATGCATGAAACACTT
NGF	TGCATAGCGTAATGTCCATGTTG	CTGTGTCAAGGGAATGCTGAA
GDNF	TTGCATTCCTGCTACAGTGC	TGTAGCTGGGCCTCCTTCTA
PGK1	ATGCAAAGACTGGCCAAGCTAC	AGCCACAGCCTCAGCATATTTC
RPL13a	GGATCCCTCCACCCTATGACA	CTGGTACTTCCACCCGACCTC
YWHAZ	GATGAAGCCATTGCTGAACTTG	GTCTCCTTGGGTATCCGATGTC
ACTB	TGTCACCAACTGGGACGATA	GGGGTGTTGAAGGTCTCAAA

with Alexa Fluor 568 and goat anti-rabbit conjugated with Alexa Fluor 568 (all used at 1:1000).

2.10. Microscopy

Images were acquired using either a fluorescence microscope (Leica DM2000 LED microscope; 2D Schwann cell cultures), inverted epi-fluorescence microscope (Nikon Eclipse Ti-e; 3D Schwann cell cultures) or a confocal laser scanning microscope (Leica TCS SP8; iPSC-Schwann cell coculture). Images were prepared and analysed using Fiji software. To quantify marker expression, we measured the mean area of each marker and corrected this for the total number of cells present. At least 10 images were taken per sample (5 replicates per condition). The VAA3D software was used to create 3D rendered images (VAA3D-Neuron2_Autotracing) (Peng et al., 2014).

2.11. Image analysis

Images were prepared and analysed using Fiji software (https://fiji.sc/). Results were analyzed in a blinded manner. To quantify marker expression in 2D samples (coverslips and well-plates) and 3D scaffolds, the positive area covered by each marker was determined by manually setting the threshold. The total area was subsequently corrected by the total number of cells in the image. Cell count was performed using the standard Analyze Particles function to DAPI + objects. At least 10 images per sample, and 5 replicates per conditions were analyzed.

To measure the axonal area, the βIII tubulin positive area occupied by the neurites was determined, thereby excluding cell bodies. Next, for the myelinated are, the MBP positive are was measured within the same area excluding the central segment of the scaffold.

2.12. Statistics

The GraphPad Prism 9.0.0 software (GraphPad software Inc) was used to analyze the data and build the subsequent graphs. All data are shown as mean ± standard error mean (SEM). If the sample size was $n \leq 4$, differences between groups were assessed by a non-parametric Mann-Whitney or Kruskal-Wallis test along with Dunn's post-hoc analysis, with the vehicle group serving as the reference. For sample sizes of $n \geq 5$, normality was verified using the Shapiro-Wilk test before conducting the analysis. Normally distributed data were subsequently analyzed with a *t*-test or one-way ANOVA with Tukey's multiple comparison. A p-value of 0.05 was considered statistically significant ($^{*}p \leq 0.05$, $^{**}p \leq 0.01$, $^{***}p \leq 0.005$, $^{****}p \leq 0.001$).

3. Results

3.1. CPT-cAMP stimulates Schwann cell differentiation

Since PDE4 inhibitors indirectly elevate intracellular cAMP levels, we first aimed to validate the role of cAMP itself on Schwann cell differentiation. Exposing primary rat Schwann cells to a cell membrane-permeable CPT-cAMP analogue (250 μM 8-(4-Chlorophenylthio)adenosine 3′,5′-cyclic monophosphate sodium salt) led to a significant enhancement of Schwann cell differentiation into a myelinating phenotype. After 3 days of CPT-cAMP administration, Schwann cells adapted a shift in both morphology and phenotype. While vehicle treated cells remained elongated, CPT-cAMP-treated Schwann cells adopted a flattened shape with a large cytoplasmic-to-nuclei ratio (Fig. 1A-B). Gene expression analysis revealed a significant upregulation of the myelin gene MBP (Fig. 1C) and a trend towards upregulation of PLP (Fig. 1D). The transcription factor Krox20, which controls Schwann cell myelination by suppressing the cJun pathway, was significantly upregulated upon CPT-cAMP treatment (Fig. 1E). Accordingly, cJun expression was significantly reduced in CPT-cAMP treated Schwann cells (Fig. 1F). The phenotypic consequences of these changes in gene expression were confirmed using immunocytochemistry (Fig. 1G). Schwann cells treated with CPT-cAMP displayed a significant upregulation of the glycolipid marker for mature myelinating cells 01, and the myelin protein MBP and MAG (Fig. 1H-J), and an increased expression of Krox20 (Fig. 1K), while cJun expression was significantly reduced (Fig. 1L).

3.2. PDE4 inhibition by roflumilast stimulates Schwann cell differentiation in both a 2D and 3D culture condition

To evaluate the effect of the PDE4 inhibitor roflumilast on cellular differentiation, primary rat Schwann cells were exposed to roflumilast (5 μM or 10 μM) for 6 days and subsequently analysed for their myelination phenotype. Similar to exogenous cAMP supplementation, roflumilast stimulated Schwann cell differentiation at both 5 μM and 10 μM exposure led to a significant upregulation of the myelin protein MBP and the glycolipid O1 (Fig. 2A-C).

Next, to assess the differentiation promoting potential of Schwann cells in a more biologically relevant model, we cultured primary Schwann cells on a 3D scaffold that induces Schwann cell alignment, mimicking the initial stages of PNS regeneration (Fig. 3A). Both 5 μM and 10 μM of roflumilast treatment significantly increased myelin gene expression (MBP, PLP and MAG) (Fig. 3B-D) and SOX10 expression, a key transcription factor of Schwann cell lineage cells (Fig. 3E). With regard to myelin protein expression (Fig. 3F), both 5 μM and 10 μM roflumilast induced a significant upregulation of both MAG and MBP on the 3D Schwann cell bands compared to the vehicle condition (Fig. 3G-

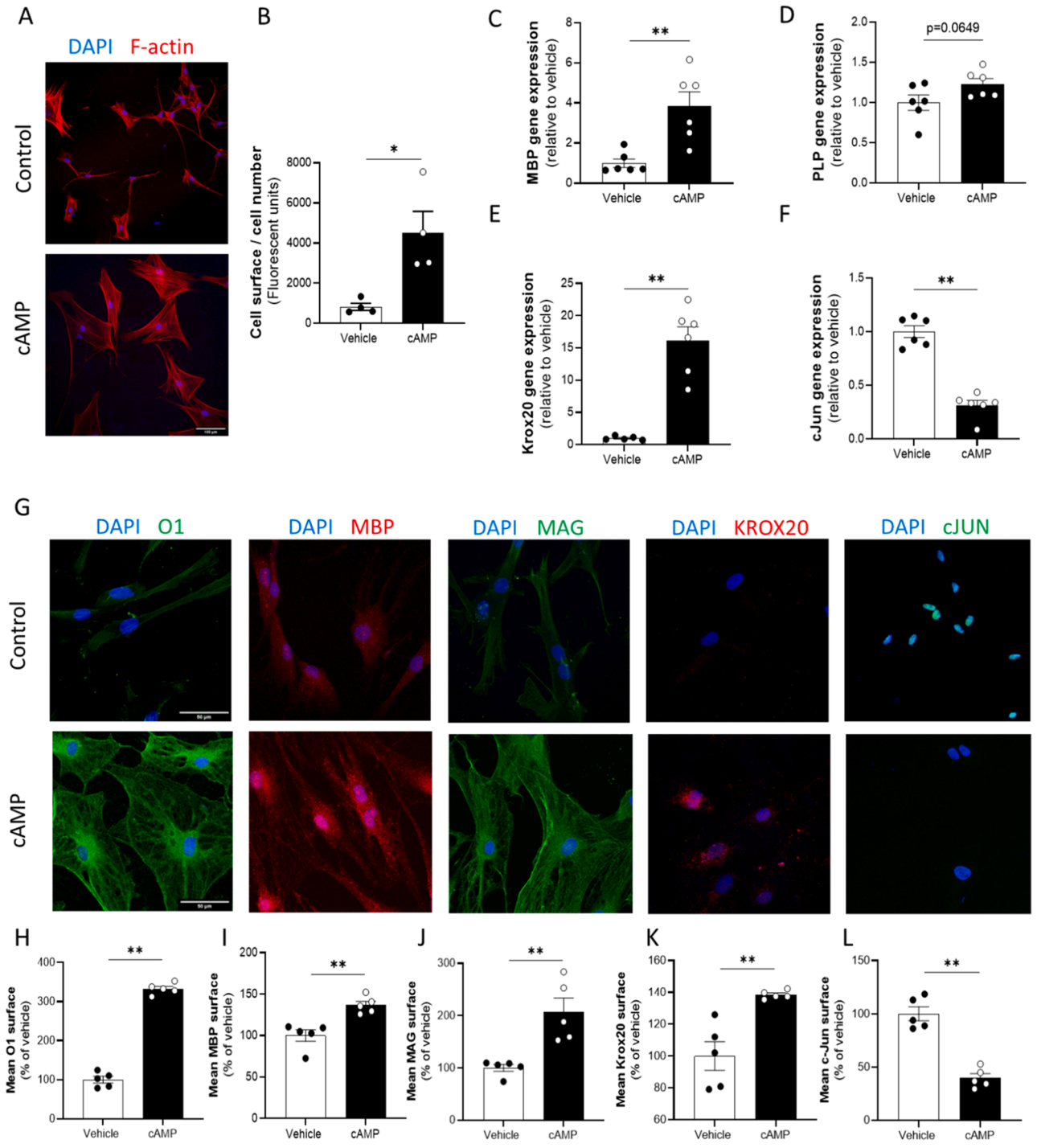

Fig. 1. CPT-cAMP boosts Schwann cell differentiation into a myelinating phenotype. Schwann cells were treated for 3 days with a CPT-cAMP analogue and subsequently evaluated for their morphology and phenotype. (A-B) Schwann cell morphology was assessed using a cytoskeletal F-actin staining which demonstrates a flattened and significantly increased cell surface upon CPT-cAMP treatment. Scale bar indicates 100 μm. (C-F) Gene expression analysis reveals a significant upregulation of the myelin gene (C) MBP, a trend towards upregulation for the myelin gene (D) PLP, a significant upregulation of the transcription factor (E) Krox20 and a significant downregulation of the transcription factor (F) cJun. (G) Immunocytochemical staining analysis demonstrates a significant upregulation of the myelin protein (H) O1, (I) MBP, and (J) MAG upon CPT-cAMP treatment. Furthermore, the (K) Krox20 protein levels were significant increased, while (L) cJun protein levels were significantly decreased. Scale bar indicates 50 μm. Data are presented as mean ± SEM ($n = 5$/group). Data were analysed using a non-parametric Mann-Whitney test. (*$p < 0.05$; **$p < 0.01$).

H).

3.3. Roflumilast treated Schwann cells showed an increased myelination speed of iPSC-derived nociceptive neurons

To evaluate whether the differentiation promoting capacity of roflumilast translates into a higher myelination capacity, we co-cultured

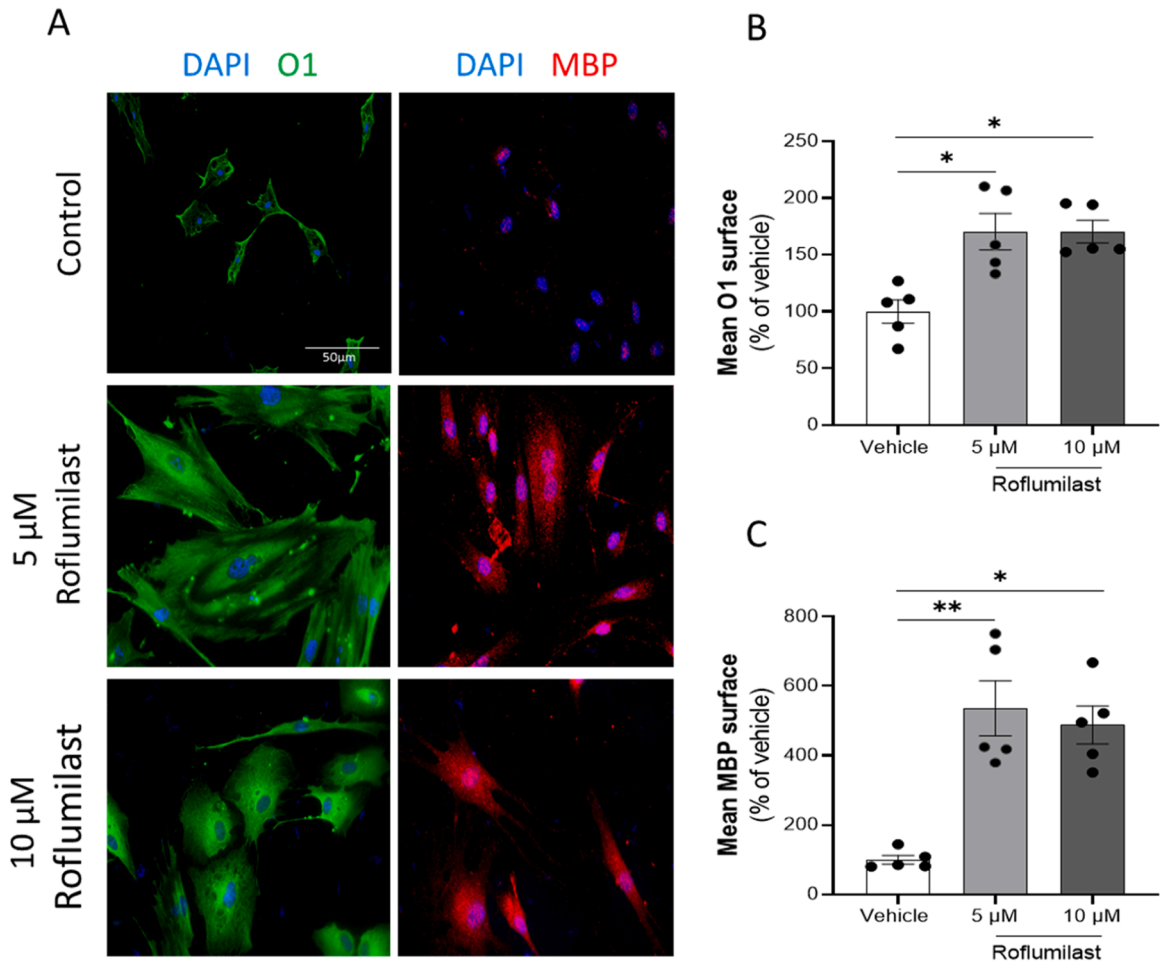

Fig. 2. Roflumilast boosts Schwann cell differentiation into a myelinating phenotype. Schwann cells were treated for 6 days with either 5 µM or 10 µM roflumilast (treatment repeated every other day) and subsequently analysed for their differentiation promoting capacity. (A) Immunocytochemical analysis revealed a significant upregulation of both (B) O1 and (C) MBP protein levels upon roflumilast treatment. Scale bars are 50 µm. Data are presented as mean ± SEM ($n = 5$/group). Data were analysed using a non-parametric Kruskal-Wallis test with Dunn's post-hoc analysis (compared to vehicle). (*$p < 0.05$; **$p < 0.01$).

rat Schwann cells with human iPSC-derived nociceptive neurons. Since we did not observed a clear discrepancy between both concentrationstested (5µM and 10µM), we subsequently decided to continue with the highest dose capable of influencing Schwann cell biology. Schwann cell alignment was first accomplished by culturing cells on the 3D scaffolds and subsequently treated with 10 µM roflumilast for 6 days (Fig. 3A). Next, iPSC-derived neurospheres were added to the Schwann cell cultures, which were maintained for 14 or 21 days in neural medium, and subsequently axonal region and myelinated area were analysed. After 14 days of coculture, roflumilast-treated Schwann cells significantly promoted axonal outgrowth of iPSC-derived neurons (Fig. 4A-B), which was accompanied with an increased myelinated area (Fig. 4A-C). After 21 days of coculture, no difference in both axonal area or myelinated area were observed (Fig. 4D-F).

3.4. The EPAC inhibitor ESI-09 inhibits myelin gene expression, while the PKA inhibitor H-89 prevents neurotrophic factor gene expression following roflumilast treatment

As demonstrated above, both cAMP and roflumilast treatment increases the maturation of primary rat Schwann cells. The expression of myelin genes, including MBP, PLP and MAG, was significantly upregulated in Schwann cells treated with db-cAMP or roflumilast compared to the control group (Fig. 5A-C). Similarly, the expression of neurotrophic factors, including brain-derived neurotrophic factor (BDNF), nerve growth factor (NGF), and glial-derived neurotrophic factor (GDNF), was significantly increased as well upon db-cAMP or roflumilast treatment (Fig. 5D-F).

To further investigate the downstream signaling pathways involved in the roflumilast-induced upregulation of myelin genes and neurotrophic factors, Schwann cells were treated with the EPAC inhibitor ESI-09 or the PKA inhibitor H-89 simultaneously with roflumilast. Co-treatment of Schwann cells with roflumilast and the EPAC inhibitor ESI-09 significantly inhibited the increase in myelin gene expression (Fig. 5A-C), whereas co-treatment with roflumilast and the PKA inhibitor H-89 significantly inhibited the increase in neurotrophic factor expression (Fig. 5D-F).

4. Discussion

PDE4 inhibitors hold promise as therapeutics for the treatment of multiple disorders. With respect to the nervous system, most reports to date have focused on CNS disorders, thereby overlooking the therapeutic potential of PDE4 inhibitors on PNS repair. In this study, we demonstrate that PDE4 inhibition, by means of roflumilast, promotes Schwann cell differentiation into a myelinating phenotype. Furthermore, Schwann cells treated with roflumilast promote axonal outgrowth of human iPSC-derived nociceptive neurons while simultaneously enhancing their myelination capacity. The findings from this study support the use of PDE4-inhibitor based treatment strategies for the treatment of peripheral demyelinating neuropathies.

It has been shown that enhancing intracellular cAMP signaling

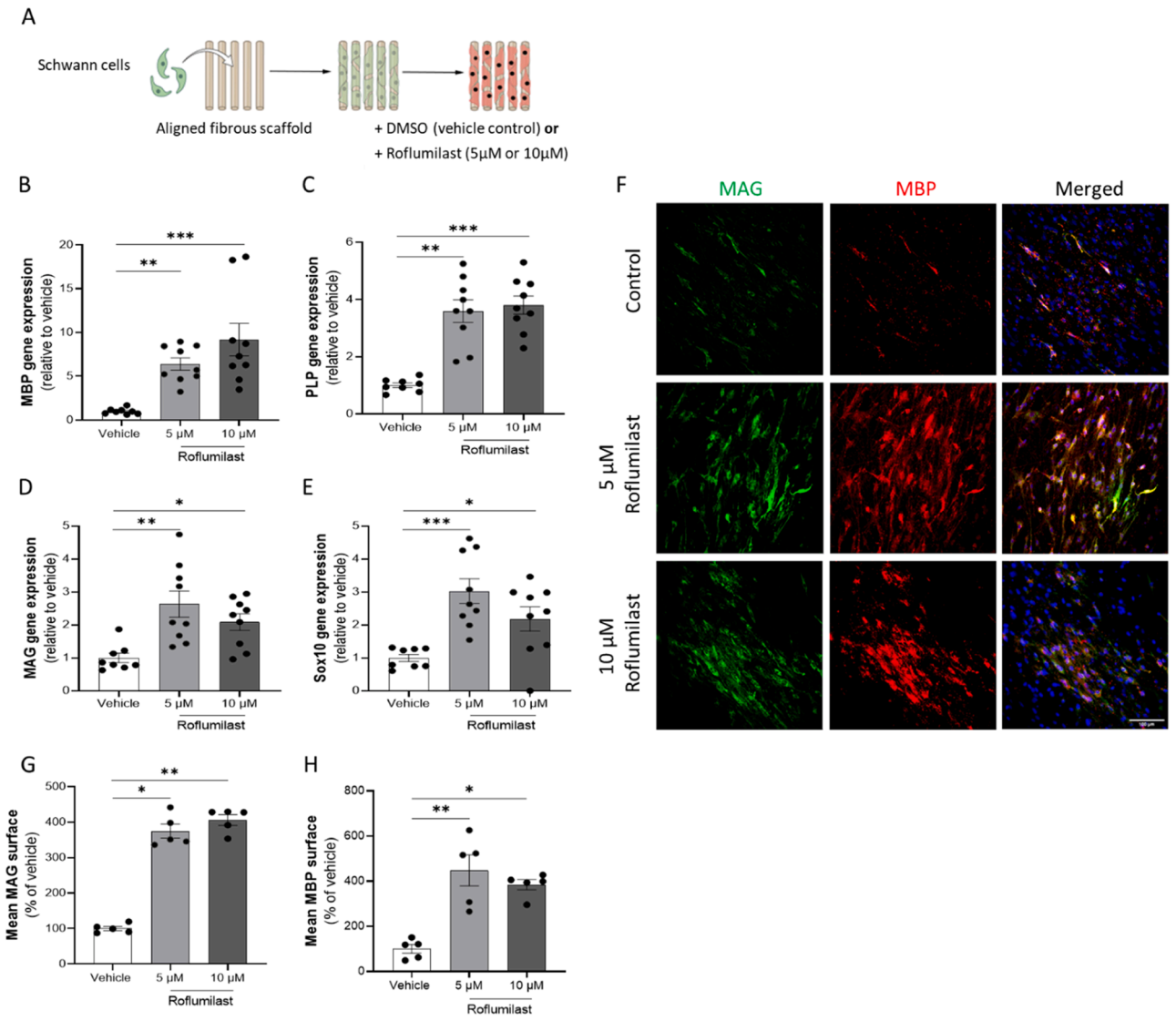

Fig. 3. Roflumilast boosts Schwann cell differentiation into a myelinating and nerve repair promoting phenotype. (A) Primary rat Schwann cells were seeded onto a 3D aligned scaffold to generate Schwann cell composed bands of Büngner mimicking regeneration bands. Cells were treated with either 5 μM or 10 μM roflumilast for 6 days (treatment repeated every other day). (B-E) Both 5 μM and 10 μM roflumilast treatment led to a significant upregulation of (B) MBP, (C) PLP, (D) MAG, and (E) SOX10 gene expression compared to vehicle treated cells. (F) Immunohistochemical analysis demonstrate a significant increase in myelin protein surface of both (G) MAG and (H) MBP. Scale bars are 100 μm. Data are presented as mean ± SEM (n = 5/group). Data were analysed using a non-parametric Kruskal-Wallis test with Dunn's post-hoc analysis (compared to vehicle). (*p < 0.05; **p < 0.01; ***p < 0.005).

promotes Schwann cell differentiation (Bacallao and Monje, 2015; Jessen et al., 1991; Monje et al., 2010; Guo et al., 2012; Knott et al., 2014). To first validate these findings, we treated primary rat Schwann cells with 250 μM of a membrane-permeable cAMP analogue, a concentration known to cause a fast and robust change in the cellular phenotype (Bacallao and Monje, 2015, 2013). Indeed, cAMP-treated Schwann cells enlarged up to 5-times compared to vehicle treated cells and increased their gene expression and protein levels of myelin genes and Krox20, while exhibiting lower levels of cJun. With regards to PDE4 inhibition in Schwann cells, the main findings so far focused on *in vivo* administration of the PDE4 inhibitor rolipram to stimulate peripheral nerve regeneration and remyelination. After surgical repair of transected nerves, a 0.4 μmol/kg/h infusion of rolipram promotes axonal outgrowth over the lesion size in rats (Udina et al., 2010). Furthermore, a daily intraperitoneal injection of 5 mg/kg rolipram has shown to rescue peripheral myelin deficiencies in Rac1-CKO mice after 8 weeks (Guo et al., 2012). Nevertheless, no compelling conclusions of PDE4 inhibition on Schwann cells specifically can be drawn from these *in vivo* findings since PDE4 inhibition has shown to also directly influence neuroregeneration and neuroplasticity (Schepers et al., 2019; Ponsaerts et al., 2021; Wang et al., 2018). In the CNS, exogenous cAMP dosing or the application of PDE4 inhibitors, such as rolipram and roflumilast, have shown to improve oligodendrocyte precursor cells (OPCs) differentiation and oligodendrocyte-mediated *de novo* myelin formation after injury (Syed et al., 2013). In this study, we show now that primary rat Schwann cells trceated with the PDE4 inhibitor roflumilast significantly increase O1 and MBP levels, indicating a phenotypical shift towards promoting myelination.

Following PNS injury, Schwann cells guide axonal outgrowth by forming aligned cellular tracks called bands of Büngner (Jessen and Mirsky, 2016; Salzer, 2015). These bands of Büngner provide a favourable cellular and molecular environment (*e.g.* laminin and collage IV secretion) that conduces regrowing axons via haptotaxis back to their target during early PNS regeneration (Jessen and Mirsky, 2016). Therefore, in a next step, a biologically relevant 3D platform was applied that topographically guides cellular alignment and promotes anisotropic

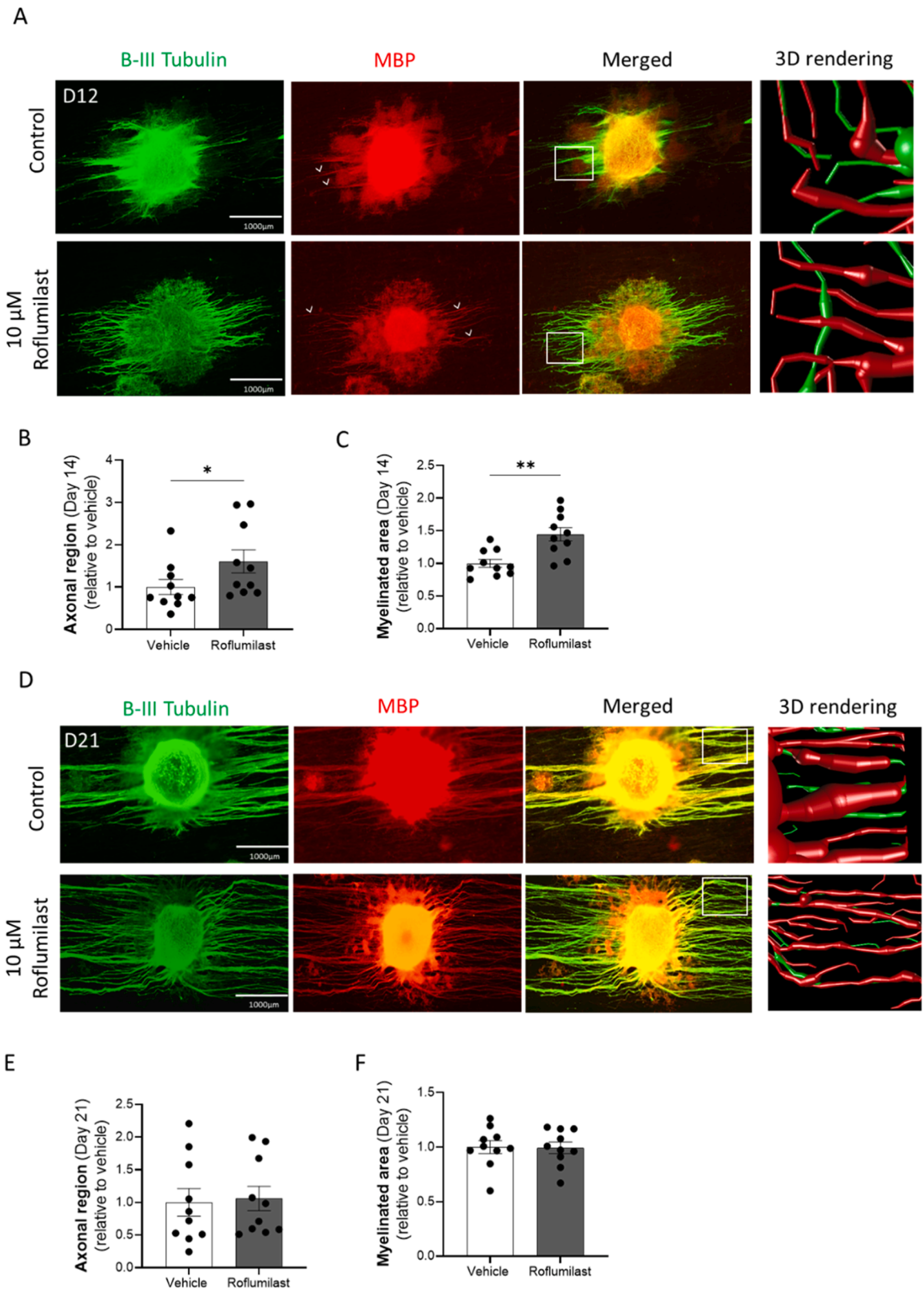

Fig. 4. Roflumilast treated Schwann cells accelerate axonal outgrowth and myelination of iPSC-derived nociceptive neurons. Schwann cells were cultured on 3D scaffolds and treated for 6 days with 10 µM roflumilast (treatment repeated every other day). Subsequently, iPSC-derived neurospheres were added to the treated Schwann cells and maintained for an additional 14 or 21 days. (A) Immunocytochemical analysis demonstrate an increased (B) axonal growth and (C) myelination of iPSC-derived neurons cultured with roflumilast treated Schwann cells after 14 days. (D) Immunohistochemical analysis showed no differences in either (E) axonal growth, nor (F) myelination following 21 days of co-culture. Arrowheads highlight myelinated axon structures. White squares indicate the 3D rendered image location. Scale bars are 1000 µm. Data are presented as mean ± SEM ($n = 10$/group). Data were analysed using a non-parametric Mann-Whitney test. (*$p < 0.05$; **$p < 0.01$).

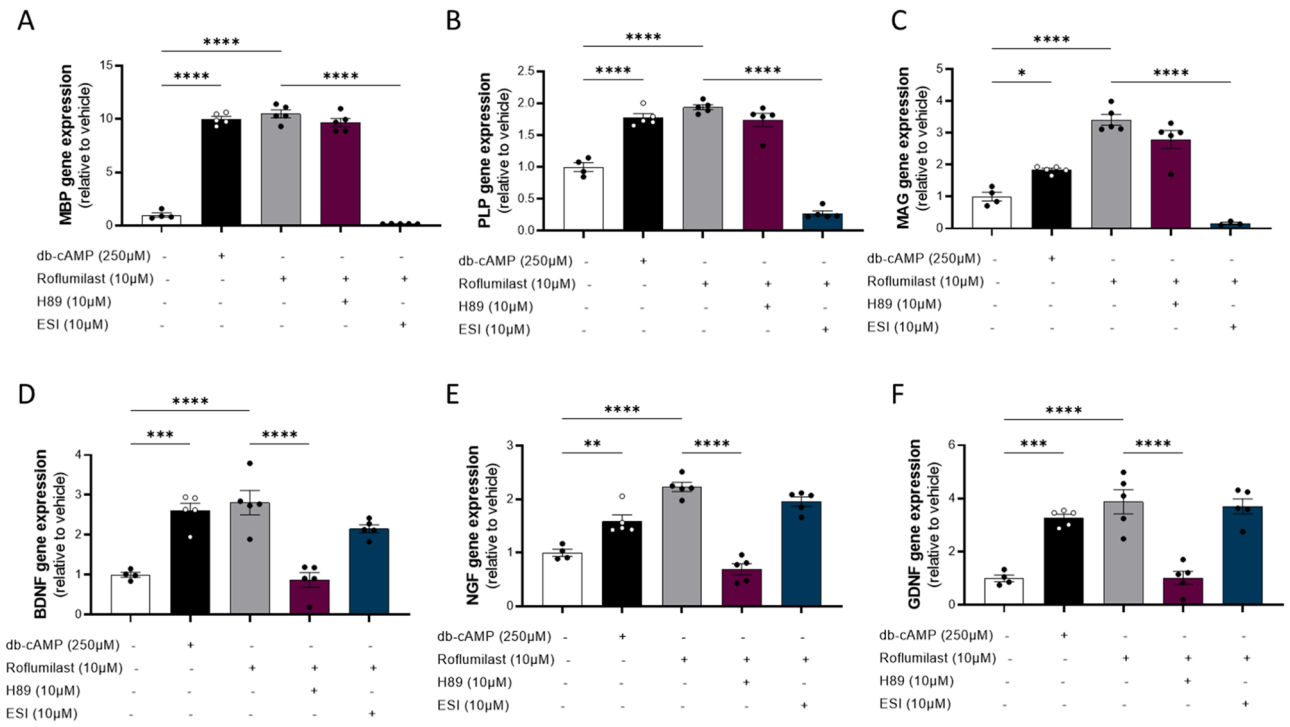

Fig. 5. Roflumilast increase myelin gene expression and neurotrophic factor gene expression via downstream EPAC and PKA signaling respectively. Schwann cells were treated for 6 days with either 250 μM db-cAMP or 10 μM roflumilast with or without 10 μM ESI-09 (EPAC inhibitor) or 10 μM H-89 (PKA inhibitor). Gene expression analysis reveals a significant upregulation of the myelin genes (A) MBP, (B) PLP and (C) MAG upon db-cAMP or roflumilast treatment, which is inhibited upon ESI-09 treatment. Additionally, neurotrophic factor gene expression, including (D) BDNF, (E) NGF and (F) GDNF was significantly upregulated following db-cAMP and roflumilast treatment which was prevented when co-treated with H89. Data are presented as mean ± SEM ($n \geq 4$/group). Data were analysed using a one-way ANOVA with Tukey's multiple comparison (*$p < 0.05$; **$p < 0.01$; ***$p < 0.005$; ****$p < 0.001$). .

Schwann cell band formation similar to the *in vivo* bands of Büngner (Malheiro et al., 2020, 2021). To test the potential of PDE4 inhibition on Schwann cell alignment, we seeded primary rat Schwann cells on the scaffold and treated them with roflumilast for 6 days. Both 5 μM and 10 μM of roflumilast demonstrated to significantly enhance myelin gene expression (MAG, MBP and PLP) and SOX10 expression, this latter being a transcription factor that confirms the Schwann cell lineage fate (Britsch et al., 2001). No significant difference was observed between both roflumilast concentrations used within this study. This indicates a non-linear dose-effect relationship between the PDE4 inhibitor and the Schwann cell differentiation, likely displaying an inverted U-shaped response. The inverted U-shape correlation creates an "area of best performance" comprising a (small) range of biologically effective dosages. Since no significant differences were observed between both 5 μM and 10 μM concentration, both roflumilast concentrations are likely to be within the "area of best performance". Importantly, the upregulation in gene expression was accompanied with an elevated protein level of the myelin proteins MAG and MBP, further confirming the increase in myelinating phenotype of Schwann cells obtained upon PDE4 inhibition.

As demonstrated in this study, the ubiquitously expressed second messenger cAMP significantly promotes Schwann cell differentiation. In addition, we demonstrate here that PDE4 inhibition, by means of roflumilast, boosts Schwann cell differentiation and promotes both myelination and axonal outgrowth of iPSC-derived neurons, this latter likely due to mitogenic growth factor secretion. Previously, it was shown that the presence and abundance of myelinated MBP positive segments positively correlated with compacted myelin layers and myelinated area as observed with transmission electron microscopy, indeed indicating a functional myelination phenotype of Schwann cells when stimulated with roflumilast (Malheiro et al., 2021). Interestingly, after 21 days of co-culture, no differences were observed in either axonal or myelinated area, indicating mainly an accelerated neurite outgrowth and myelination promoting effect of PDE4 inhibition. Besides myelination, Schwann cells have been reported to support axonal growth directly via the secretion of mitogenic growth factors (*e.g.* neuregulin), another process controlled by cAMP signaling (Jessen et al., 1991; Morgan et al., 1991; Sobue and Pleasure, 1984; Raff et al., 1978). The outcome of cAMP signaling in Schwann cells highly depends on the set of downstream effectors activated. Increasing intracellular cAMP levels activates a downstream signaling cascade involving, among others, protein kinase A (PKA), cyclic nucleotide-gated ion channels and exchange protein directly activated by cAMP (EPAC) (Sanders and Rajagopal, 2020; Li et al., 2018). These downstream effectors are involved in regulating several physiological processes, including immunomodulation, glial cell differentiation and neural regeneration (Tibbo et al., 2019; Udina et al., 2010; Li et al., 2018). In Schwann cells, the mitogenic activity of cAMP exclusively relies on downstream PKA signaling, while the differentiation boosting action relies on a PKA-independent mechanism partially involving EPAC signaling (Monje, 2015; Bacallao and Monje, 2013). By preventing the degradative action of PDE4 enzymes, intracellular levels of cAMP can be raised, activating both PKA and EPAC downstream signaling. In this study, we demonstrated that both db-cAMP and the PDE4 inhibitor roflumilast were effective in boosting the expression of myelin genes (MBP, PLP, and MAG) and genes related to neurotrophic factors (BDNF, NGF, and GDNF) in primary rat Schwann cells. Interestingly, when downstream EPAC was inhibited, the expression of myelin genes was hindered after PDE4 inhibition, while the inhibition of PKA significantly impeded the expression of neurotrophic factor genes. The difference in downstream EPAC and PKA signaling provides valuable insights into how stimulation of the cAMP pathway can support both neurite outgrowth and myelination simultaneously.

Unfortunately, high levels of PDE4 inhibition *in vivo* coincide with emetic side effects such as vomiting and nausea, hampering their direct

translation towards a clinical application (Paes et al., 2021). However, current research in the area of PNS repair has involved the creating of nerve guidance conduits (NGCs) which are pre-seeded with Schwann cells to enhance the regenerative process (Parker et al., 2021). The results we show here suggest that PDE4 inhibition could be applied *ex vivo* to SC-laden NGCs in order to prime their regenerative phenotype further, thereby achieving enhanced nerve repair in the first critical days after injury, while avoiding a systemic application of inhibitors that can lead to emesis. Alternatively, the PDE4 family comprises four PDE4 subtypes, PDE4A-D, and selective ablation of any of the PDE4 subtypes did not result in emetic side effects, rending PDE4 subtype inhibition a novel and safe therapeutic avenue to explore (McDonough et al., 2020). Identifying and targeting the specific PDE4 subtype responsible for Schwann cell differentiation can therefore hold the key for comprising therapeutic benefits, without inducing emetic side effects (Schepers et al., 2023). Whether or not the remyelination and mitogenic growth factor secretion of PDE4 inhibition to boost PNS regeneration is within the emetic dose range of a drug remains to be elucidated. However, based on previous *in vivo* studies evaluating the effect of the PDE4 inhibitor rolipram, of which the emetogenic profile is known, it is highly likely that the therapeutic dose is accompanied with emetic side effect (Vanmierlo et al., 2016). Identifying the PDE4 subtype responsible for the regenerative therapeutic properties can therefore lower the occurrence of potential adverse side effects and therefore increase their therapeutic potential.

Taken together, our data demonstrate that pharmacological PDE4 inhibition by roflumilast promotes Schwann cell differentiation into a myelinating phenotype. Furthermore, roflumilast-treated Schwann cells increase axonal outgrowth of iPSC-derived nociceptive neurons. These *in vitro* findings provide a new incentive for future *in vivo* studies investigating the potential of PDE4 inhibitors to treat PNS neuropathies, thereby further aiding drug development for pursuing new and improved PNS regenerative therapies.

Author contribution

MS, AM, ASG, NH, JP, LM, TV, and PW conceived the research design. MS and AM performed the experiments and subsequent data analysis. MS and AM wrote the manuscript with input from all authors. All authors read and approved the final manuscript.

Data availability

Data will be made available on request.

Acknowledgments

TV, JP and MS have proprietary interest in selective PDE4D inhibitors for the treatment of demyelinating disorders.

We thank the Microscopy CORE Lab (M4I Maastricht University), especially Hans Duimel and Kevin Knoops for their help in confocal imaging. We thank the province of Limburg for the project funding. This work was partly supported by the research program VENI 2017 STW-project 15900 financed by the Dutch Research Council (NWO), the FWO (12G0817N and 1S57521N) and the Fondation Charcot Stichting.

References

Bacallao, K., Monje, P.V., 2013. Opposing roles of PKA and EPAC in the cAMP-dependent regulation of schwann cell proliferation and differentiation [corrected]. PLoS One 8 (12), e82354.

Bacallao, K., Monje, P.V., 2015. Requirement of cAMP signaling for Schwann cell differentiation restricts the onset of myelination. PLoS ONE 10 (2), e0116948.

Balakrishnan, A., Belfiore, L., Chu, T.H., Fleming, T., Midha, R., Biernaskie, J., et al., 2020. Insights into the role and potential of schwann cells for peripheral nerve repair from studies of development and injury. Front. Mol. Neurosci. 13, 608442.

Britsch, S., Goerich, D.E., Riethmacher, D., Peirano, R.I., Rossner, M., Nave, K.A., et al., 2001. The transcription factor Sox10 is a key regulator of peripheral glial development. Genes Dev. 15 (1), 66–78.

Chambers, S.M., Qi, Y., Mica, Y., Lee, G., Zhang, X.J., Niu, L., et al., 2012. Combined small-molecule inhibition accelerates developmental timing and converts human pluripotent stem cells into nociceptors. Nat. Biotechnol. 30 (7), 715–720.

Glenn, T.D., Talbot, W.S., 2013. Analysis of Gpr126 function defines distinct mechanisms controlling the initiation and maturation of myelin. Development 140 (15), 3167–3175.

Guo, L., Moon, C., Niehaus, K., Zheng, Y., Ratner, N., 2012. Rac1 controls Schwann cell myelination through cAMP and NF2/merlin. J. Neurosci. 32 (48), 17251–17261.

Han, S.H., Yun, S.H., Shin, Y.K., Park, H.T., Park, J.I., 2019. Heat shock protein 90 is required for cAMP-induced differentiation in rat primary Schwann cells. Neurochem. Res. 44 (11), 2643–2657.

Han, S.H., Kim, Y.H., Park, S.J., Cho, J.G., Shin, Y.K., Hong, Y.B., et al., 2023. COUP-TFII plays a role in cAMP-induced Schwann cell differentiation and *in vitro* myelination by up-regulating Krox20. J. Neurochem.

Hatzelmann, A., Morcillo, E.J., Lungarella, G., Adnot, S., Sanjar, S., Beume, R., et al., 2010. The preclinical pharmacology of roflumilast–a selective, oral phosphodiesterase 4 inhibitor in development for chronic obstructive pulmonary disease. Pulm. Pharmacol. Ther. 23 (4), 235–256.

Jessen, K.R., Mirsky, R., 2016. The repair Schwann cell and its function in regenerating nerves. J. Physiol. 594 (13), 3521–3531.

Jessen, K.R., Mirsky, R., Morgan, L., 1991. Role of cyclic AMP and proliferation controls in Schwann cell differentiation. Ann. N. Y. Acad. Sci. 633, 78–89.

Jessen, K.R., 2004. Glial cells. Int. J. Biochem. Cell Biol. 36 (10), 1861–1867.

Kaewkhaw, R., Scutt, A.M., Haycock, J.W., 2012. Integrated culture and purification of rat Schwann cells from freshly isolated adult tissue. Nat. Protoc. 7 (11), 1996–2004.

Knott, E.P., Assi, M., Pearse, D.D., 2014. Cyclic AMP signaling: a molecular determinant of peripheral nerve regeneration. Biomed. Res. Int. 2014, 651625.

Li, H., Zuo, J., Tang, W., 2018. Phosphodiesterase-4 inhibitors for the treatment of inflammatory diseases. Front. Pharmacol. 9, 1048.

Malheiro, A., Morgan, F., Baker, M., Moroni, L., Wieringa, P., 2020. A three-dimensional biomimetic peripheral nerve model for drug testing and disease modelling. Biomaterials 257, 120230.

Malheiro, A., Harichandan, A., Bernardi, J., Seijas-Gamardo, A., Konings, G.F., Volders, P.G.A., et al., 2021. 3D culture platform of human iPSCs-derived nociceptors for peripheral nerve modeling and tissue innervation. Biofabrication 14 (1).

McDonough, W., Aragon, I.V., Rich, J., Murphy, J.M., Abou Saleh, L., Boyd, A., et al., 2020. PAN-selective inhibition of cAMP-phosphodiesterase 4 (PDE4) induces gastroparesis in mice. FASEB J. 34 (9), 12533–12548.

Monje, P.V., Rendon, S., Athauda, G., Bates, M., Wood, P.M., Bunge, M.B., 2009. Non-antagonistic relationship between mitogenic factors and cAMP in adult Schwann cell re-differentiation. Glia 57 (9), 947–961.

Monje, P.V., Soto, J., Bacallao, K., Wood, P.M., 2010. Schwann cell dedifferentiation is independent of mitogenic signaling and uncoupled to proliferation: role of cAMP and JNK in the maintenance of the differentiated state. J. Biol. Chem. 285 (40), 31024–31036.

Monje, P.V., 2015. To myelinate or not to myelinate: fine tuning cAMP signaling in Schwann cells to balance cell proliferation and differentiation. Neural Regen. Res. 10 (12), 1936–1937.

Morgan, L., Jessen, K.R., Mirsky, R., 1991. The effects of cAMP on differentiation of cultured Schwann cells: progression from an early phenotype (04+) to a myelin phenotype (P0+, GFAP-, N-CAM-, NGF-receptor-) depends on growth inhibition. J. Cell Biol. 112 (3), 457–467.

Nikulina, E., Tidwell, J.L., Dai, H.N., Bregman, B.S., Filbin, M.T., 2004. The phosphodiesterase inhibitor rolipram delivered after a spinal cord lesion promotes axonal regeneration and functional recovery. Proc. Natl. Acad. Sci. U. S. A. 101 (23), 8786–8790.

Paes, D., Schepers, M., Rombaut, B., van den Hove, D., Vanmierlo, T., Prickaerts, J., 2021. The molecular biology of phosphodiesterase 4 enzymes as pharmacological targets: an interplay of isoforms, conformational states, and inhibitors. Pharmacol. Rev. 73 (3), 1016–1049.

Parker, B.J., Rhodes, D.I., O\`Brien, C.M., Rodda, A.E., Cameron, N.R, 2021. Nerve guidance conduit development for primary treatment of peripheral nerve transection injuries: a commercial perspective. Acta Biomater. 135, 64–86.

Parkinson, D.B., Bhaskaran, A., Arthur-Farraj, P., Noon, L.A., Woodhoo, A., Lloyd, A.C., et al., 2008. c-Jun is a negative regulator of myelination. J. Cell Biol. 181 (4), 625–637.

Peng, H., Bria, A., Zhou, Z., Iannello, G., Long, F., 2014. Extensible visualization and analysis for multidimensional images using Vaa3D. Nat. Protoc. 9 (1), 193–208.

Ponsaerts, L., Alders, L., Schepers, M., de Oliveira, R.M.W., Prickaerts, J., Vanmierlo, T., et al., 2021. Neuroinflammation in Ischemic Stroke: inhibition of cAMP-Specific Phosphodiesterases (PDEs) to the Rescue. Biomedicines 9 (7).

Raff, M.C., Hornby-Smith, A., Brockes, J.P., 1978. Cyclic AMP as a mitogenic signal for cultured rat Schwann cells. Nature 273 (5664), 672–673.

Salzer, J.L., 2015. Schwann cell myelination. Cold Spring Harb. Perspect. Biol. 7 (8), a020529.

Sanders, O., Rajagopal, L., 2020. Phosphodiesterase inhibitors for alzheimer\'s disease: a systematic review of clinical trials and epidemiology with a mechanistic rationale. J. Alzheimers Dis. Rep. 4 (1), 185–215.

Schepers, M., Tiane, A., Paes, D., Sanchez, S., Rombaut, B., Piccart, E., et al., 2019. Targeting phosphodiesterases-towards a tailor-made approach in multiple sclerosis treatment. Front. Immunol. 10, 1727.

Schepers, M., Paes, D., Tiane, A., Rombaut, B., Piccart, E., van Veggel, L., et al., 2023. Selective PDE4 subtype inhibition provides new opportunities to intervene in neuroinflammatory *versus* myelin damaging hallmarks of multiple sclerosis. Brain Behav. Immun. 109, 1–22.

Sobue, G., Pleasure, D., 1984. Schwann cell galactocerebroside induced by derivatives of adenosine 3′,5′-monophosphate. Science 224 (4644), 72–74.

Sun, X., Liu, Y., Liu, B., Xiao, Z., Zhang, L, 2012. Rolipram promotes remyelination possibly via MEK-ERK signal pathway in cuprizone-induced demyelination mouse. Exp. Neurol. 237 (2), 304–311.

Syed, Y.A., Baer, A., Hofer, M.P., Gonzalez, G.A., Rundle, J., Myrta, S., et al., 2013. Inhibition of phosphodiesterase-4 promotes oligodendrocyte precursor cell differentiation and enhances CNS remyelination. EMBO Mol. Med. 5 (12), 1918–1934.

Tibbo, A.J., Tejeda, G.S., Baillie, G.S., 2019. Understanding PDE4′s function in Alzheimer \'s disease; a target for novel therapeutic approaches. Biochem. Soc. Trans. 47 (5), 1557–1565.

Udina, E., Ladak, A., Furey, M., Brushart, T., Tyreman, N., Gordon, T., 2010. Rolipram-induced elevation of cAMP or chondroitinase ABC breakdown of inhibitory proteoglycans in the extracellular matrix promotes peripheral nerve regeneration. Exp. Neurol. 223 (1), 143–152.

Vanmierlo, T., Creemers, P., Akkerman, S., van Duinen, M., Sambeth, A., De Vry, J., et al., 2016. The PDE4 inhibitor roflumilast improves memory in rodents at non-emetic doses. Behav. Brain Res. 303, 26–33.

Walikonis, R.S., Poduslo, J.F., 1998. Activity of cyclic AMP phosphodiesterases and adenylyl cyclase in peripheral nerve after crush and permanent transection injuries. J. Biol. Chem. 273 (15), 9070–9077.

Wang, H., Gaur, U., Xiao, J., Xu, B., Xu, J., Zheng, W., 2018. Targeting phosphodiesterase 4 as a potential therapeutic strategy for enhancing neuroplasticity following ischemic stroke. Int. J. Biol. Sci. 14 (12), 1745–1754.

Yamada, H., Komiyama, A., Suzuki, K., 1995. Schwann cell responses to forskolin and cyclic AMP analogues: comparative study of mouse and rat Schwann cells. Brain Res. 681 (1–2), 97–104.